# Clathrin mediates integrin endocytosis for focal adhesion disassembly in migrating cells

Ellen J. Ezratty, Claire Bertaux, Eugene E. Marcantonio, and Gregg G. Gundersen

Department of Pathology and Cell Biology, Columbia University, New York, NY 10032

Focal adhesion disassembly is regulated by microtubules (MTs) through an unknown mechanism that involves dynamin. To test whether endocytosis may be involved, we interfered with the function of clathrin or its adaptors autosomal recessive hypercholesteremia (ARH) and Dab2 (Disabled-2) and found that both treatments prevented MT-induced focal adhesion disassembly. Surface labeling experiments showed that integrin was endocytosed in an extracellular matrix–, clathrin-, and ARH- and Dab2-dependent manner before entering Rab5 endosomes. Clathrin colocalized with a subset of focal adhesions in an ARH- and Dab2-dependent fashion. Direct imaging showed that clathrin rapidly accumulated on focal adhesions during MT-stimulated disassembly and departed from focal adhesions with integrin upon their disassembly. In migrating cells, depletion of clathrin or Dab2 and ARH inhibited focal adhesion disassembly and decreased the rate of migration. These results show that focal adhesion disassembly occurs through a targeted mechanism involving MTs, clathrin, and specific clathrin adaptors and that direct endocytosis of integrins from focal adhesions mediates their disassembly in migrating cells.

## Introduction

Directional cell migration is a fundamental process required for embryonic development, inflammation, wound healing, cancer metastasis, and atherosclerosis (Lauffenburger and Horwitz, 1996; Ridley et al., 2003). A key aspect of directional migration of well-adherent cells is the establishment of transient attachments to the ECM through integrin clusters that form plaques known as focal adhesions. Focal adhesions establish a connection between the ECM and the actin cytoskeleton and serve as points of traction for the cell. The contraction of focal adhesion–associated actin stress fibers is thought to propel the cell body forward.

As the cell migrates, integrin clustering induces the formation of small focal adhesions (also referred to as focal contacts) at the front of the cell. Some of these nascent focal adhesions mature into larger focal adhesions, whereas others are rapidly turned over. Whether nascent focal adhesions disassemble or become mature focal adhesions depends on Rho-regulated myosin contractility (Rottner et al., 1999; Webb et al., 2004; Gupton and Waterman-Storer, 2006). Mature focal adhesions are selectively disassembled in the cell body so that few remain in the tail (Abercrombie, 1980; Smilenov et al., 1999). The disassembly of focal adhesions is important to allow for tail retraction, and integrin detachment from the ECM is rate limiting for cell migration in several cases (Hendey et al., 1992; Palecek et al., 1997).

In contrast to well-established mechanisms for focal adhesion formation (for reviews see Sastry and Burridge, 2000; Webb et al., 2002), the mechanisms for focal adhesion disassembly are not well understood. Focal adhesions in the tail of the cell may be disassembled or left on the substratum in processes that are regulated by calpain (Palecek et al., 1998) and Rho (Worthylake et al., 2001). Microtubules (MTs) also contribute to focal adhesion disassembly by delivering a relaxing factor whose nature is unknown (Kaverina et al., 1999). In none of these cases is it clear how focal adhesion disassembly is

Correspondence to Gregg G. Gundersen: ggg1@columbia.edu

E.J. Ezratty's present address is Laboratory of Mammalian Cell Biology and Development, The Rockefeller University, New York, NY 10065.

E.E. Marcantonio's present address is Merck Research Laboratories, Merck and Co., Rahway, NJ 07065.

Abbreviations used in this paper: ARH, autosomal recessive hypercholesteremia; FKBP, FK506-binding protein 12; GAPDH, glyceraldehyde 3-phosphate dehydrogenase; LC, light chain; MT, microtubule; TIRF, total internal reflection fluorescence.



The Rockefeller University Press $30.00
J. Cell Biol. Vol. 187 No. 5 733–747
www.jcb.org/cgi/doi/10.1083/jcb.200904054

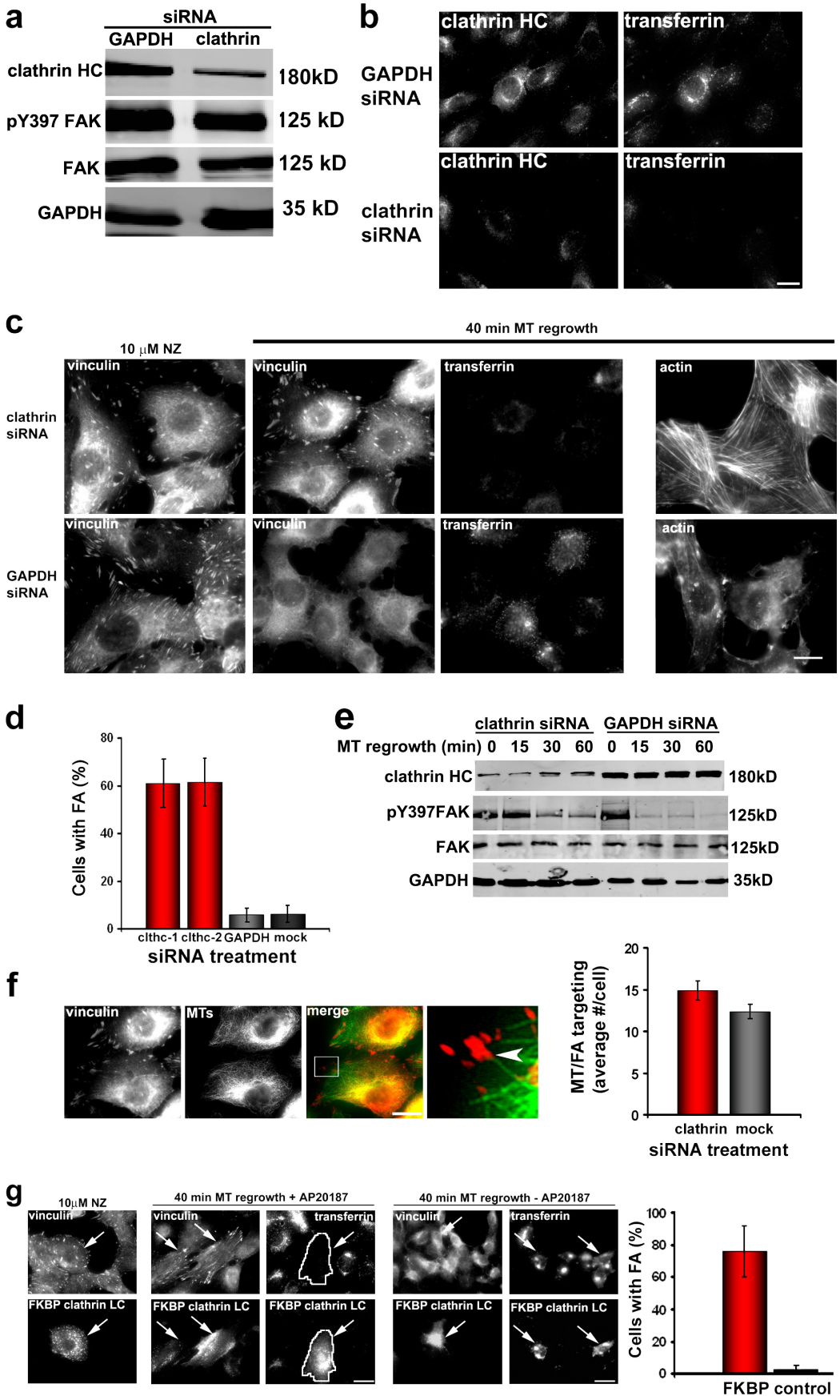


Figure 1. **Clathrin is required for MT-induced focal adhesion disassembly.** (a) Western blot of clathrin heavy chain (HC) siRNA– or GAPDH siRNA–treated NIH3T3 fibroblasts showing levels of clathrin heavy chain, FAK, pY397 FAK, and GAPDH. (b) Clathrin heavy chain immunofluorescence and transferrin

spatially regulated to target some focal adhesions for disassembly while others remain intact.

The fate of integrins after focal adhesion disassembly is also unknown. Experiments have suggested that a proportion of integrins from the tail are left behind on the substratum (Palecek et al., 1996). Other studies have suggested that integrins travel through vesicular intermediates and endomembrane compartments (Lawson and Maxfield, 1995; Palecek et al., 1996; Pierini et al., 2000). In these experiments, integrin trafficking was correlated with cell migration, but the relationship between focal adhesion disassembly and the fate of the integrin was not clearly established. Nonetheless, a prevailing idea is that the formation and disassembly of focal adhesions during cell migration are coupled to the recycling of integrins through endocytic processes. This idea is supported by evidence that general integrin recycling can contribute to cell migration (Caswell and Norman, 2006; Pellinen and Ivaska, 2006; Nishimura and Kaibuchi, 2007) and that integrins are endocytosed into Rab-labeled endocytic compartments during growth factor stimulation of cells (Roberts et al., 2001; Pellinen et al., 2006).

Focal adhesion disassembly occurs in a common cytoplasm along with focal adhesion formation, and there are few systems in which disassembly can be studied independently of assembly. We developed an assay that kinetically separates focal adhesion disassembly from assembly based on our finding that MT regrowth after nocodazole washout induced synchronous disassembly of focal adhesions. MT-induced focal adhesion disassembly was dependent on FAK and dynamin but was independent of active Rho and Rho-regulated contractility (Ezratty et al., 2005). MTs and dynamin are also involved in the turnover of podosomes, adhesive structures in macrophages, and other hematopoietic cells that are related to focal adhesions (Bruzzaniti et al., 2005; Kopp et al., 2006). Dynamin's canonical role in the scission of vesicles during endocytosis raises the possibility that endocytosis may be involved in focal adhesion and podosome disassembly (Burridge, 2005).

In this study, we examine whether endocytosis of integrins regulates focal adhesion disassembly by exploring the role of clathrin in MT-induced focal adhesion disassembly. We find that clathrin is involved in focal adhesion disassembly and that clathrin accumulates at focal adhesions and departs with integrin during focal adhesion disassembly. We also show that the clathrin adaptors, Dab2 (Disabled-2) and autosomal recessive hypercholesteremia (ARH) target clathrin to focal adhesions and participate in the disassembly process. Our study supports a new mechanism for focal adhesion disassembly involving MT-stimulated endocytosis of integrins at focal adhesions.

## Results

### Clathrin is required for MT-induced focal adhesion disassembly

We first tested general inhibitors of clathrin-dependent endocytosis. Potassium depletion, which inhibits clathrin-mediated endocytosis, inhibited focal adhesion disassembly (unpublished data). To test specifically whether clathrin is required for focal adhesion disassembly, we reduced clathrin heavy chain expression using siRNA. Clathrin protein was diminished by >80% in cells treated with clathrin siRNA without affecting the levels of focal adhesion components FAK or vinculin (Fig. 1 a and not depicted). As previously reported (Moskowitz et al., 2005), transferrin uptake was inhibited in clathrin-depleted cells (Fig. 1 b). MT-induced focal adhesion disassembly was inhibited by clathrin depletion compared with untreated cells or control (glyceraldehyde 3-phosphate dehydrogenase [GAPDH]) depletion (Fig. 1 c and Fig. S1 a). Consistent with the inhibition of focal adhesion disassembly, cells depleted of clathrin still maintained stress fibers after MT regrowth, whereas cells depleted of GAPDH completely disassembled stress fibers (Fig. 1 c). Two clathrin siRNAs reduced clathrin levels and inhibited MT-induced focal adhesion disassembly, showing that there were no off-target effects (Fig. 1 d and Fig. S1 c). Quantification of focal adhesion disassembly using either a cell by cell assay (cells with <10 focal adhesions were scored as having disassembled focal adhesions) or quantitative measurements of focal adhesion number showed that clathrin depletion inhibited focal adhesion disassembly by 60–80% (Fig. 1 d and Fig. S1 b). Focal adhesion disassembly measured biochemically by monitoring levels of pY397 FAK, a FAK phosphorylation site which depends on focal adhesion (Ezratty et al., 2005; Yeo et al., 2006), showed that clathrin-depleted cells maintained pY397 FAK after MT regrowth compared with untreated cells (Ezratty et al., 2005) or control-depleted cells (Fig. 1 e). Depletion of clathrin heavy chain did not visually disrupt MTs, the rate of MT regrowth (not depicted), nor the proper targeting of MTs to focal adhesions, as assessed visually or with a quantitative assay (Fig. 1 f).

uptake in GAPDH- and clathrin heavy chain–depleted NIH3T3 fibroblasts. (c) Immunofluorescence of vinculin, actin, and transferrin uptake during MT-induced focal adhesion disassembly in GAPDH- and clathrin heavy chain–depleted NIH3T3 fibroblasts. Images are before MT regrowth (10 µM nocodazole [NZ] for 4 h) and 40 min after nocodazole washed out and MT regrowth. (d) Quantification of focal adhesion (FA) disassembly in clathrin heavy chain (clthc)–, GAPDH-, or mock-depleted NIH3T3 fibroblasts. Cells were scored positive if they retained 10 focal adhesions after MT-induced disassembly. Data are from five independent experiments in which several hundred cells were analyzed for each condition in each experiment. (e) Western blot of clathrin heavy chain, pY397 FAK, total FAK, and GAPDH during MT regrowth after nocodazole washout in cells depleted of either clathrin or GAPDH. Cells were treated with nocodazole for 4 h, and then the drug was washed out, and MTs were allowed to regrow for the indicated times before preparing samples for SDS-PAGE. (f) Immunofluorescence of vinculin and MTs after nocodazole washout (40 min) in cells depleted of clathrin. The region outlined by the box in the merged panel is shown at higher magnification at the right. The arrowhead indicates a focal adhesion targeted by an MT. The histogram shows the number of MT–focal adhesion targeting events in clathrin- or mock-depleted cells. Data are from two experiments in which 20 cells were analyzed per condition. (g) Vinculin immunofluorescence and transferrin uptake in cells expressing FKBP–clathrin LC–GFP (arrows) and treated with or without AP20187. Images shown are before (10 µM nocodazole) and 40 min after MT regrowth. The cell expressing FKBP–clathrin LC is outlined in white to show that it does not endocytose transferrin. The histogram shows quantification of focal adhesion disassembly in FKBP-LC versus nontransfected cells. (d, f, and g) Error bars are SEM. Bars, 15 µm.

Long-term depletion of clathrin by siRNA could inhibit focal adhesion disassembly indirectly by altering protein-trafficking pathways. To test this possibility, we acutely disrupted clathrin function by expressing a cross-linkable FK506-binding protein 12 (FKBP)–clathrin light chain (LC) fusion protein that oligomerizes upon addition of the dimeric rapamycin derivative AP20187 (Clackson et al., 1998). This approach rapidly and specifically inhibits clathrin by disrupting assembly and disassembly of clathrin lattices and inhibits transferrin endocytosis (Moskowitz et al., 2003). Focal adhesion disassembly and transferrin uptake were inhibited in an AP20187-dependent fashion in cells expressing FKBP–clathrin LC (Fig. 1 g). Almost 80% of cells transfected with FKBP–clathrin LC and treated with AP20187 were inhibited in focal adhesion disassembly (Fig. 1 g). Combined with the clathrin depletion experiments, these data indicate that clathrin is required for most focal adhesion disassembly induced by MTs.

### α5β1 integrin is internalized during MT-induced focal adhesion disassembly

The clathrin and dynamin (Ezratty et al., 2005) dependence of focal adhesion disassembly suggests that integrins are endocytosed during the process. To examine this possibility, we followed cell surface α5β1 integrin, the major ECM receptor engaged at focal adhesions formed on fibronectin in NIH3T3 fibroblasts. We labeled surface α5β1 integrin using fluorescent α5 integrin antibody and quantified surface α5 integrin levels by flow cytometry (see Materials and methods). Surface α5 integrin decreased almost 50% during MT regrowth after nocodazole washout, returning to almost the same level observed in cells before nocodazole treatment (Fig. 2 a and Fig. S2 a). The loss of surface integrin correlated well with the time course of focal adhesion disassembly. Surface levels of the collagen receptor subunit α1 integrin, which is not clustered in focal adhesions in cells adhering to fibronectin, remained unchanged during MT regrowth, showing that only integrin engaged by the ECM was affected by MT regrowth (Fig. 2 b and Fig. S2 a). Because total α5 integrin did not change during MT regrowth (Fig. S2 f), we conclude that ECM-bound α5 integrin is specifically endocytosed during focal adhesion disassembly. Consistent with this idea, clathrin depletion inhibited the loss of surface α5 integrin during MT regrowth relative to control-depleted cells (Fig. 2 c and Fig. S2, d and e). These results imply that only focal adhesion–associated integrin is internalized during MT-induced disassembly.

Bulk integrin endocytosed during growth factor stimulation transits through Rab5- and Rab11-positive compartments before being recycled (Roberts et al., 2001; Pellinen et al., 2006). To test whether internalized integrin transits through Rab5 endosomes during MT-induced focal adhesion disassembly, cells were transfected with constitutively active Rab5Q79L to enlarge early endosomes (Stenmark et al., 1994) and then focal adhesion disassembly was stimulated by MT regrowth. Expression of Rab5Q79L did not affect MT-stimulated focal adhesion disassembly (unpublished data). Before MT regrowth, only a small subset of the enlarged Rab5Q79L endosomes contained integrin (Fig. 2 d). However, after MT regrowth and focal adhesion disassembly, many of the Rab5Q79L endosomes contained β1 integrin (Fig. 2 d). The extent of colocalization of β1 integrin with Rab5-positive endosomes increased more than twofold after focal adhesion disassembly (Fig. 2 e). We also observed that after MT-induced focal adhesion disassembly, β1 integrin accumulated in a perinuclear compartment that colocalized with internalized transferrin and partially with Rab11, suggesting that the integrin internalized during MT regrowth traffics through an endocytic recycling compartment (Fig. 2 f). These data further support the idea that integrin travels through endocytic compartments after focal adhesion disassembly.

### Clathrin accumulates at focal adhesions during MT-induced focal adhesion disassembly

To explore how clathrin might participate in focal adhesion disassembly, we examined the localization and dynamics of clathrin before and during MT-induced focal adhesion disassembly. By epifluorescence microscopy with antibodies against clathrin heavy chain, clathrin was observed in a perinuclear region corresponding to the Golgi as well as throughout the cytoplasm and the plasma membrane, as reported previously (Fig. 1 b). To visualize plasma membrane–associated clathrin, we used total internal reflection fluorescence (TIRF) microscopy, which only excites the ventral ∼100 nm of the cell. Localization of endogenous clathrin heavy chain by TIRF microscopy revealed typical clathrin puncta on the ventral surface of the cell with some puncta clustered and colocalized with focal adhesions (Fig. 3 a). Clathrin puncta decorated 64% of focal adhesions ($n = 250$) and covered 30–35% of the total focal adhesion area (Fig. S3) but only 4.5% of the total ventral membrane area (not depicted). Interestingly, clathrin localization at focal adhesions increased slowly during the several hours of nocodazole treatment we used to completely break down MTs (Fig. S3).

The localization data showed that clathrin is present on a subset of focal adhesions, so we next explored clathrin dynamics in living cells to address two questions: (1) do focal adhesions that exhibit clathrin colocalization disassemble during MT regrowth, and (2) do focal adhesions that lack clathrin colocalization before MT regrowth acquire clathrin during their disassembly? For these experiments, we used a cell line stably expressing GFP–clathrin LC that had also been transiently transfected with RFP-FAK. A typical example of a focal adhesion that had accumulated clathrin before MT regrowth is shown in Fig. 3 b. The focal adhesion disassembled during MT regrowth, as judged by loss of FAK fluorescence over a 15-min interval, which is consistent with disassembly intervals from previous studies (Kaverina et al., 1999; Ezratty et al., 2005). In almost every case (22/24), focal adhesions that had accumulated clathrin over at least 20% of their area before MT regrowth disassembled when MTs were regrown. Clathrin puncta on these focal adhesions dynamically rearranged as the focal adhesion disassembled (Fig. 3 b). Despite the relatively high clathrin colocalization on these focal adhesions before MT regrowth, quantification showed that overall clathrin levels increased 2.3-fold on average during disassembly (Fig. 3, c and f).

To address the second question, we imaged focal adhesions that had low levels of clathrin colocalization before

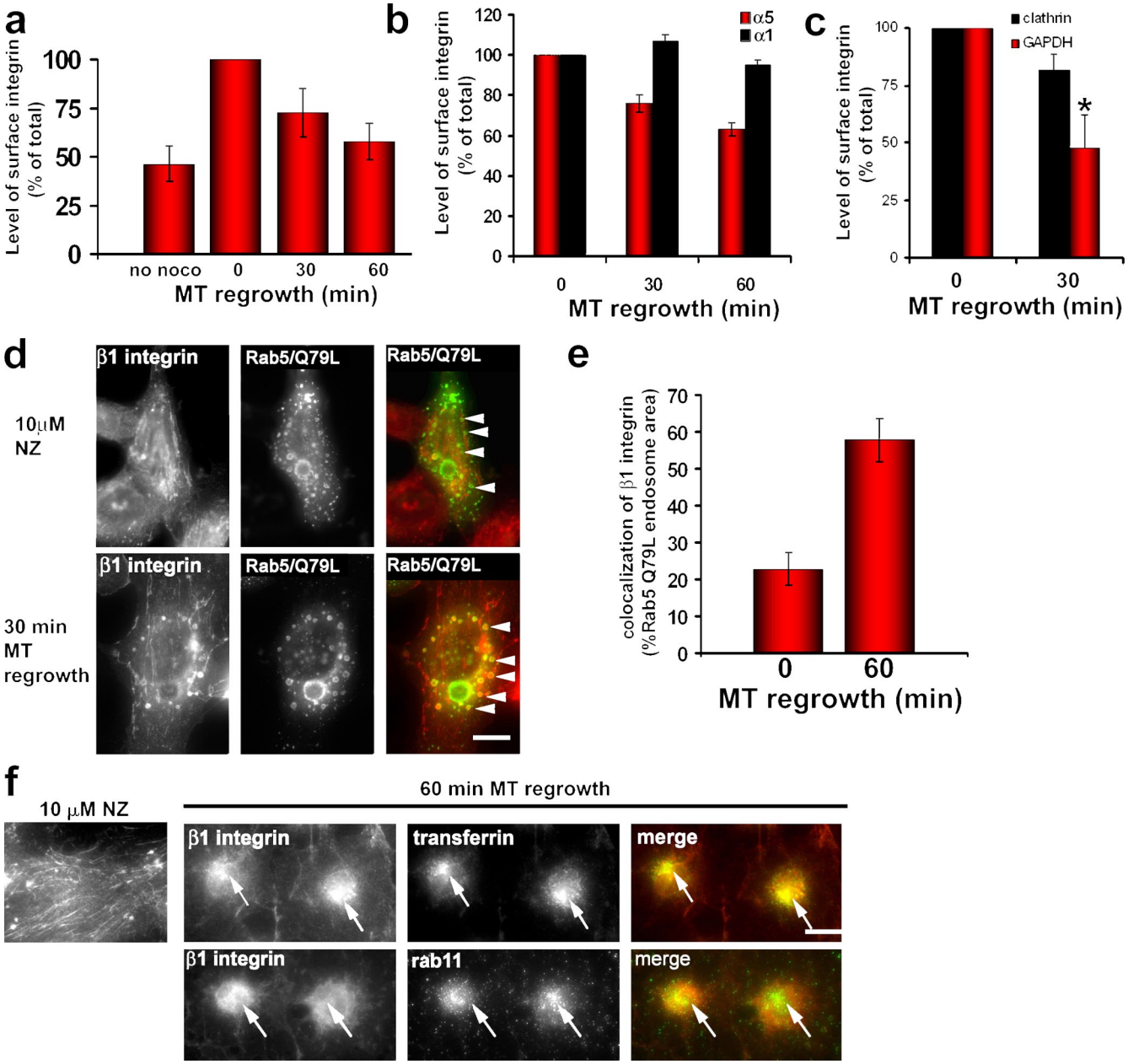


Figure 2. **α5β1 integrin is internalized by a clathrin- and ECM-dependent mechanism during MT-induced focal adhesion disassembly.** (a) Surface α5 integrin levels in NIH3T3 cells measured by flow cytometry before (no nocodazole [noco]) and during MT-induced focal adhesion disassembly. The histogram represents mean fluorescent intensity for each sample normalized to the value at 0 min MT regrowth. Data are from three independent experiments. (b) Comparison of surface α5 and α1 integrin levels in HA1 NIH3T3 cells measured by flow cytometry during MT-induced focal adhesion disassembly. The histogram represents the mean fluorescent intensity for each sample normalized to the value at 0 min MT regrowth. Data are from two independent experiments. (c) Levels of surface α5 integrin in NIH3T3 cells depleted of either clathrin or GAPDH and stimulated for MT-induced focal adhesion disassembly. The histogram represents the mean fluorescent intensity normalized to the value at 0 min MT regrowth. Data are the mean of three independent experiments. *, $P < 0.01$ by Student's *t* test. (d) Immunofluorescence of β1 integrin in NIH3T3 fibroblasts transiently transfected with Rab5Q79L-GFP and treated with 10 μM nocodazole (NZ) or after 30 min of MT regrowth. Arrowheads in the top panel indicate Rab5Q79L-GFP endosomes that do not contain internalized integrin; arrowheads in the bottom panel indicate Rab5Q79L-GFP endosomes that contain internalized integrin. (e) Quantification of the extent of colocalization of β1 integrin with Rab5Q79L-GFP–positive endosomes at 0 and 60 min of MT regrowth. The histogram represents two independent experiments in which 10 cells were analyzed for each condition. (f) Immunofluorescence of β1 integrin accumulation in a transferrin- and Rab11-positive compartment during MT-induced focal adhesion disassembly. The left panel shows β1 integrin in nocodazole-treated cells. Panels on the right show β1 integrin colocalization with internalized transferrin or Rab11 in a perinuclear compartment 60 min after MT regrowth. Arrows indicate β1 integrin colocalizing with transferrin (top) or Rab11 (bottom). (a–c and e) Error bars are SEM. Bars, 15 μm.

MT regrowth. Virtually all of these focal adhesions showed a dramatic accumulation (17.4-fold; $n = 35$) of clathrin puncta during the early periods of MT regrowth (Fig. 3, d and f). For example, the large focal adhesion shown in Fig. 3 d exhibited a 16.6-fold increase in clathrin colocalization during MT regrowth and a peak of clathrin fluorescence during its disassembly (Fig. 3 e). In contrast, clathrin did not accumulate at focal adhesions imaged in cells maintained in nocodazole (in which focal

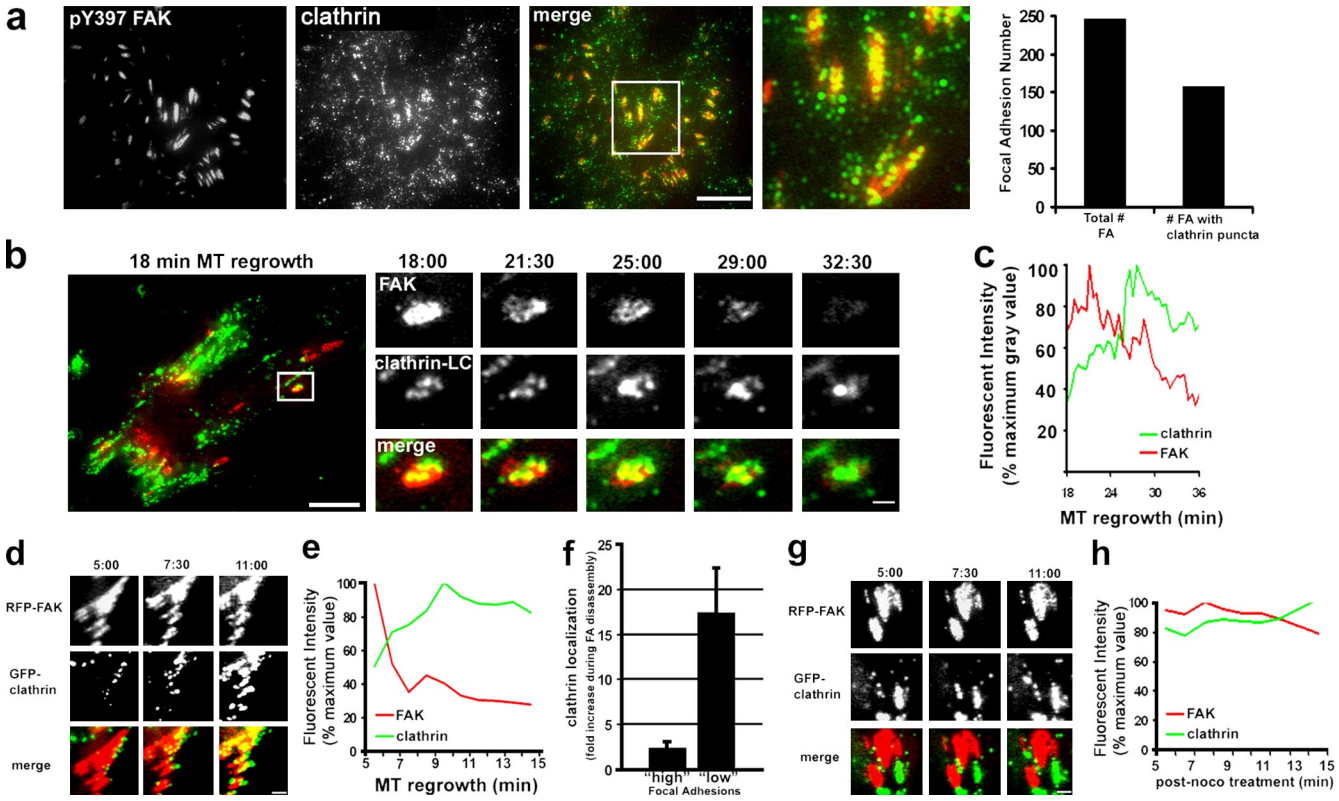


Figure 3. **Clathrin localization and dynamics during MT-induced focal adhesion disassembly.** (a) TIRF image of a nocodazole-treated NIH3T3 fibroblast immunostained with antibodies against pY397 FAK and clathrin heavy chain. The merged image shows pY397 FAK (red) and clathrin (green). The region outlined by the box is shown at higher magnification on the right. The histogram shows the number of focal adhesions with clathrin puncta. (b) The left panel shows a merged TIRF image of an NIH3T3 cell line stably expressing GFP-clathrin (green) and transiently transfected with RFP-FAK (red) 18 min after MT regrowth to stimulate focal adhesion disassembly. The outlined region is shown at higher magnification in the panels on the right during time points after MT regrowth (minutes:seconds). Note that clathrin puncta colocalize with and accumulate on the disassembling focal adhesion. (c) Quantification of clathrin and FAK fluorescence during disassembly of the focal adhesion shown in b. (d) TIRF images from a video of GFP-clathrin accumulation at focal adhesions initially devoid of clathrin during MT regrowth in RFP-FAK–expressing cells as in b. Time is in minutes:seconds after MT regrowth. (e) Quantification of clathrin and FAK fluorescence during disassembly of the large focal adhesion in the top row of d. (f) Histogram indicating the fold clathrin accumulation during disassembly of focal adhesions (FA) initially containing low or high levels of clathrin before MT regrowth. Data are from 25–30 focal adhesions. Error bars are SEM. (g) TIRF images from a video of GFP-clathrin and focal adhesions (RFP-FAK) in a cell treated with nocodazole for 4 h and imaged while still in nocodazole. Time is in minutes:seconds. (h) Quantification of clathrin and FAK fluorescence of the large focal adhesion in the top row of g. noco, nocodazole. Bars: (a, b [insets], d, and g) 2 µm; (b) 15 µm.

adhesions are not disassembling), showing that the rapid accumulation of clathrin was MT dependent (Fig. 3, g and h). These experiments show that clathrin accumulates at focal adhesions during their disassembly and reveal a previously unknown MT-dependent targeting of clathrin to focal adhesions.

### Clathrin endocytoses integrin during focal adhesion disassembly

To determine whether clathrin mediated endocytosis of integrin during focal adhesion disassembly, we imaged clathrin dynamics in cells stably expressing a GFP–β1 integrin chimera. We previously used this integrin chimera in a study of focal adhesion disassembly (Ezratty et al., 2005), and other experiments have shown that it is a faithful reporter for integrins at focal adhesions (Smilenov et al., 1999). Previous studies have used TIRF microscopy to identify the internalization of single clathrin-coated structures and their cargoes from the plasma membrane by virtue of their simultaneous disappearance from the evanescent field (Merrifield et al., 2002; Ehrlich et al., 2004; Puthenveedu and von Zastrow, 2006). Because it was difficult to observe integrin loss from the densely labeled focal adhesions at early stages of disassembly, we focused on focal adhesions that were disassembling after intermediate times of MT regrowth and therefore contained patches of integrin (Fig. 4 a). To catch individual clathrin events, we acquired images at a higher rate (every 20 s) than in our earlier videos of clathrin targeting to focal adhesions (Fig. 3). In a typical video acquired at this higher frame rate, a clathrin puncta can be seen to be recruited to a patch of β1 integrin in a disassembling focal adhesion, colocalize with β1 integrin, and then disappear simultaneously with the β1 integrin (Fig. 4 b). The integrin appeared to concentrate in the clathrin puncta during its residence at the focal adhesion (frames 11:00–11:40). Fig. 4 c shows another example of codisappearance of β1 integrin and clathrin puncta from the evanescent field during focal adhesion disassembly. Of the clathrin puncta that were colocalized with β1 integrin in disassembling focal adhesions, 57% were dynamic and disappeared from the evanescent field during the 10 min of imaging (Fig. 4 d). In more than two thirds of the cases, the departure of clathrin puncta was coincident with the loss of β1 integrin

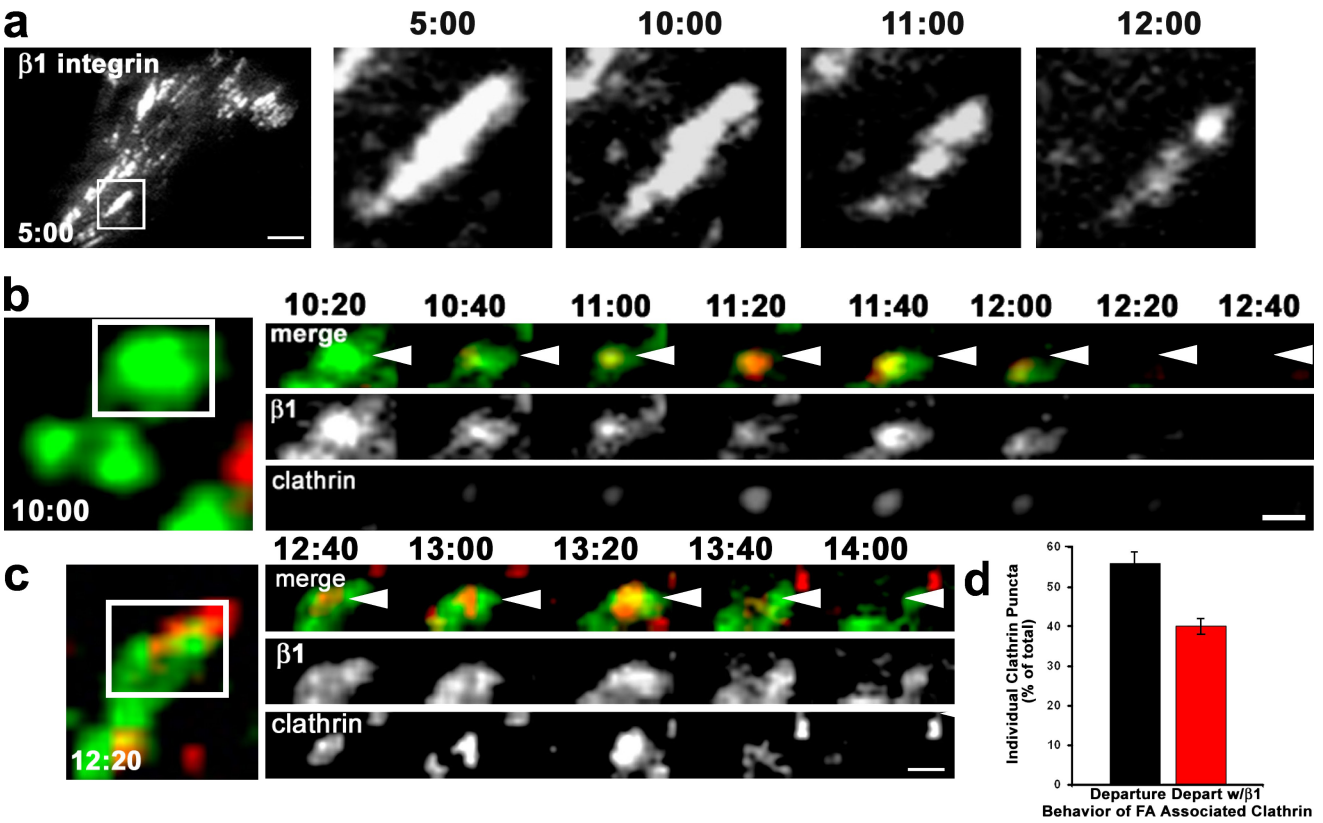


Figure 4. **Direct imaging of clathrin and β1 integrin during focal adhesion disassembly.** (a) TIRF imaging of GFP–β1 integrin during MT-induced focal adhesion disassembly. Time is in minutes:seconds after nocodazole washout. The boxed region is shown magnified at various time points in the panels on the right. (b and c) Montages from TIRF imaging of DsRed-clathrin and GFP–β1 integrin during focal adhesion disassembly. Time is in minutes:seconds. The boxed areas are depicted in the panels on the right. In the merged panels, arrowheads point to clathrin/β1 integrin puncta that colocalize and then simultaneously disappear. (d) Quantification of the behavior of β1 integrin–associated clathrin puncta. The histogram represents data from 30 focal adhesions in four different videos, in which 50 individual clathrin puncta were analyzed during focal adhesion (FA) disassembly. Error bars are SEM. Bars: (a) 10 μm; (b and c) 2 μm.

from the focal adhesion (Fig. 4, b–d). In the remaining cases, no loss of β1 integrin was detected with the departing clathrin, which may reflect abortive disassembly of clathrin coats, as has been seen in other experiments (Puthenveedu and von Zastrow, 2006). These data indicate that clathrin can directly mediate the endocytosis of β1 integrin at the focal adhesion during MT-induced focal adhesion disassembly.

### The alternate clathrin adaptors Dab2 and ARH are localized at focal adhesions

Clathrin is recruited to endocytic targets via interactions with adaptor molecules that have binding sites for clathrin and specific endocytic targets (Traub, 2003). To determine whether clathrin adaptors targeted clathrin to focal adhesions, we first examined the localization of the major clathrin adaptor AP-2 in nocodazole-treated cells and found little colocalization with focal adhesions by TIRF microscopy (Fig. 5, a and b). Transferrin uptake is AP-2 dependent and is blocked by a dominant-negative version of the accessory protein Eps15 (Benmerah et al., 2000). Consistent with the lack of AP-2 colocalization with focal adhesions, expression of dominant-negative Eps15 blocked transferrin uptake but did not affect focal adhesion disassembly (Fig. S4).

We next determined whether the alternate clathrin adaptors numb, Dab2, and ARH were localized at focal adhesions. These proteins comprise the set of known clathrin adaptors that contain a phosphotyrosine-binding domain, which interacts with the nonphosphorylated NPXY endocytic motifs in the cytoplasmic domain of certain receptors, including β integrin subunits (Calderwood et al., 2003; Uhlik et al., 2005). A screen of these adaptors revealed that Dab2 puncta accumulated in focal adhesions, whereas numb, ARH, and AP-2 were largely excluded from focal adhesions (Fig. 5 a). Quantification showed that Dab2 colocalized with 35% of the total focal adhesion area in nocodazole-treated cells, whereas numb, ARH, and AP-2 colocalized with <6% of the total focal adhesion area (Fig. 5 b). Virtually all of the clathrin puncta at focal adhesions colocalized with Dab2 (Fig. 5 c), and 68% of focal adhesions ($n$ = 100) showed colocalization of both clathrin and Dab2. We occasionally detected Dab2 puncta at focal adhesions that did not colocalize with clathrin (unpublished data). These results suggest that Dab2 may be the primary adaptor protein that targets clathrin to the focal adhesion. This idea would be consistent with evidence that Dab2 binds the cytoplasmic tail of integrins in vitro and coimmunoprecipitates with β1 integrin in vivo (Calderwood et al., 2003; Prunier and Howe, 2005).

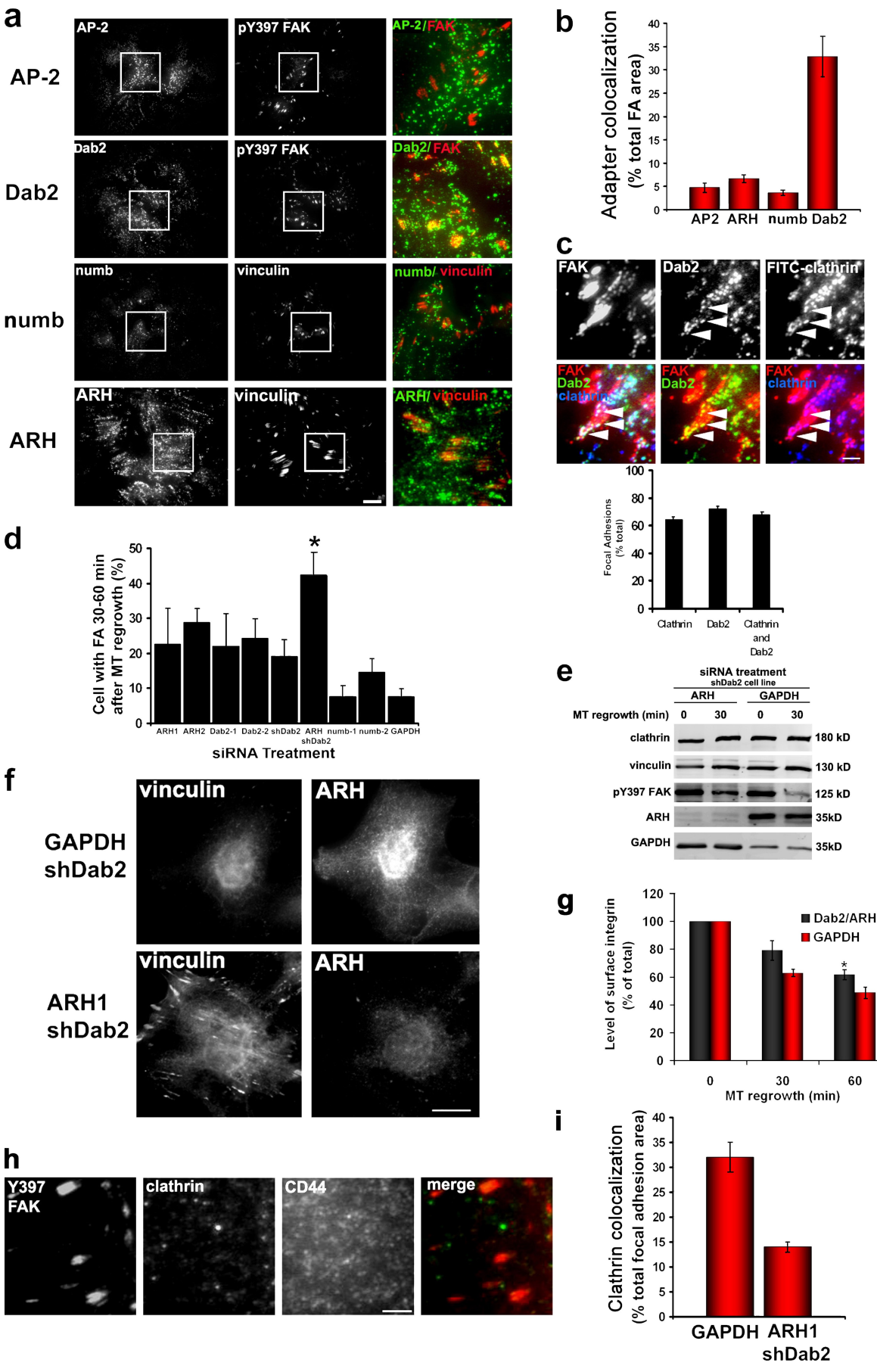
a
AP-2
Dab2
numb
ARH
AP-2
pY397 FAK
AP-2/FAK
Dab2
pY397 FAK
Dab2/FAK
numb
vinculin
numb/ vinculin
ARH
vinculin
ARH/ vinculin
b
Adapter colocalization (% total FA area)
AP2 ARH numb Dab2
c
FAK
Dab2
FITC-clathrin
FAK Dab2 clathrin
FAK Dab2
FAK clathrin
Focal Adhesions (% total)
Clathrin
Dab2
Clathrin and Dab2
d
Cell with FA 30-60 min after MT regrowth (%)
ARH1 ARH2 Dab2-1 Dab2-2 shDab2 ARH shDab2 numb-1 numb-2 GAPDH
siRNA Treatment
e
siRNA treatment
shDab2 cell line
ARH
GAPDH
MT regrowth (min) 0 30 0 30
clathrin 180 kD
vinculin 130 kD
pY397 FAK 125 kD
ARH 35kD
GAPDH 35kD
f
GAPDH shDab2
ARH1 shDab2
vinculin
ARH
g
Level of surface integrin (% of total)
Dab2/ARH
GAPDH
MT regrowth (min)
h
Y397 FAK
clathrin
CD44
merge
i
Clathrin colocalization (% total focal adhesion area)
GAPDH ARH1 shDab2

### Dab2 and ARH are involved in clathrin targeting to focal adhesions and focal adhesion disassembly

We used siRNA knockdown to test whether Dab2, ARH, or numb was required for MT-induced focal adhesion disassembly. Two different specific siRNA duplexes that reduced proteins levels at least 80% were used for each adaptor molecule (Fig. 5 e and not depicted). Individual depletion of Dab2 or ARH partially inhibited focal adhesion disassembly, whereas depletion of numb had almost no effect compared with the GAPDH control (Fig. 5 d). We also stably depleted Dab2 in cell lines by expressing a short hairpin directed against Dab2 (shDab2). In two cell lines in which the levels of Dab2 were reduced by >80% compared with controls (Fig. S5 a), focal adhesion disassembly was inhibited only by ~20% (Fig. 5 d). ARH is a distant relative of Dab2, and both proteins have been shown to play a functionally redundant role in low density lipoprotein receptor internalization (Keyel et al., 2006). Given this potential functional redundancy, we used siRNA to deplete ARH in the shDab2 cell lines. Focal adhesion disassembly was inhibited in >40% of the cells depleted of both Dab2 and ARH (Fig. 5, d and f). In contrast, focal adhesion disassembly was inhibited in ~20% of cells depleted of either adaptor protein alone. Inhibition of focal adhesion disassembly by simultaneous ARH and Dab2 knockdown but not by Dab2 knockdown alone was also evident with the biochemical marker pY397 FAK (Fig. 5 e). Simultaneous depletion of ARH and Dab2 also inhibited the loss of cell surface α5 integrin during MT regrowth (Fig. 5 g). These data suggest that Dab2 and ARH function additively during MT-induced focal adhesion disassembly and integrin endocytosis.

To test whether these adaptor proteins were involved in recruiting clathrin to the focal adhesion, we localized clathrin in cells depleted of these proteins. Individual knockdown of either adaptor protein alone did not alter the localization of clathrin to focal adhesions (Fig. S5 b and not depicted). Strikingly, ARH redistributed to focal adhesions upon depletion of Dab2, which may explain why cells depleted of Dab2 have persistent focal adhesion–associated clathrin (Fig. S5 c). In cells simultaneously depleted of Dab2 and ARH, clathrin localization to focal adhesions was reduced by >50% (Fig. 5, h and i). Clathrin levels remained unchanged by Dab2 and ARH depletion (Fig. 5 e). Collectively, these results indicate that ARH and Dab2 contribute to the targeting of clathrin to focal adhesions and focal adhesion disassembly.

### Clathrin and its adaptors accumulate at a subset of focal adhesions in migrating cells

Next, we examined the localization of clathrin and its adaptors during cell migration, during which focal adhesion disassembly occurs in a physiological context. In unperturbed cells migrating into an in vitro wound, clathrin puncta were observed at a subset of focal adhesions (Fig. 6 a). The most prominent colocalization of clathrin was with large focal adhesions in the midregion of the cell; fewer clathrin puncta were found in focal adhesions close to the leading edge. We quantified the regional colocalization of clathrin with focal adhesions by dividing the cell into four regions evenly spaced along the leading edge–tail axis (Fig. 6 b). Clathrin colocalized with 30% of the focal adhesion area in zone 2 but only 8–12% of the focal adhesion area in other regions of migrating cells (Fig. 6 c). In contrast, only 2% of the total ventral plasma membrane area contained clathrin puncta, indicating that clathrin is specifically concentrated at certain focal adhesions.

Quantification of the colocalization of the adaptors at focal adhesions showed that Dab2, and to a lesser extent ARH, colocalized with a high percentage of focal adhesions in region 2 of migrating cells (Fig. 6, d and e). Interestingly, both Dab2 and ARH also showed relatively high levels of colocalization with focal adhesions in regions 1 and 3, regions in which clathrin colocalization was relatively low. The accumulation of Dab2 and ARH in focal adhesions was specific as numb did not show appreciable accumulation in any region of the cell (Fig. 6 e). These results demonstrate that clathrin and specific clathrin adaptors are localized in specific focal adhesions in migrating fibroblasts. Combined with an earlier study, which showed that disassembly of large focal adhesions occurred predominantly in the midregion of migrating cells (Smilenov et al., 1999), these results are consistent with the idea that these molecules are involved in focal adhesion disassembly during cell migration.

Figure 5. **Clathrin adaptors Dab2 and ARH localize to focal adhesions and are required for MT-induced focal adhesion disassembly and recruitment of clathrin to focal adhesions.** (a) TIRF images of NIH3T3 fibroblasts treated with 10 μM nocodazole for 4 h and immunostained with antibodies against either pY397 FAK or vinculin and the indicated clathrin adaptors. Boxed regions are shown at higher magnification in the merged images in the panels on the right. (b) Quantification of adaptor protein colocalization with focal adhesion (FA) area in nocodazole-treated cells. The histogram represents data from two independent experiments in which colocalization was measured in 10–20 individual cells. (c) TIRF images of NIH3T3 fibroblasts treated with 10 μM nocodazole for 4 h and immunostained with antibodies against pY397 FAK, Dab2, and clathrin. The bottom row shows merged images as indicated. Arrowheads point to individual puncta of Dab2 and clathrin that colocalize at the focal adhesion. Data in the histogram show the percentage of focal adhesions with clathrin, Dab2, or clathrin and Dab2 colocalization. (d) Quantification of focal adhesion disassembly in NIH3T3 fibroblasts treated with the indicated siRNAs or short hairpin RNAs. The histogram represents data from three independent experiments in which several hundred cells were analyzed per condition. For ARH/Dab2: *, P = 0.004 by two-tailed Student's *t* test compared with GAPDH. For individual ARH, Dab2, or numb: P > 0.2 (two-tailed Student's *t* test compared with GAPDH). (e) Western blot of pY397 FAK during MT regrowth after nocodazole washout in an shDab2 cell line depleted of either ARH or GAPDH with siRNAs. Cells were treated for 4 h with nocodazole, and then the drug was washed out, and MTs were allowed to regrow for the indicated time. Vinculin is shown as a loading control. (f) Immunofluorescence of vinculin and ARH in an shDab2 cell line depleted of GAPDH or ARH by siRNA and stimulated for focal adhesion disassembly by MT regrowth for 60 min. (g) Levels of surface α5 integrin in NIH3T3 cells depleted of either Dab2 and ARH or GAPDH and stimulated for MT-induced focal adhesion disassembly. The histogram represents the mean fluorescent intensity normalized to the value at 0 min of MT regrowth. Data are averaged from five independent experiments. *, P = 0.003 by Student's *t* test. (h) TIRF images of shDab2 cell line depleted of ARH and immunostained for pY397 FAK, clathrin heavy chain, or CD44 to visualize the plasma membrane. (i) Quantification of clathrin colocalization with focal adhesion area in shDab2 cells depleted of either GAPDH or ARH by siRNA. The histogram represents two experiments in which 15 cells were analyzed for each condition. (b–d, g, and i) Error bars are SEM. Bars: (a, f, and h) 15 μm; (c) 1 μm.

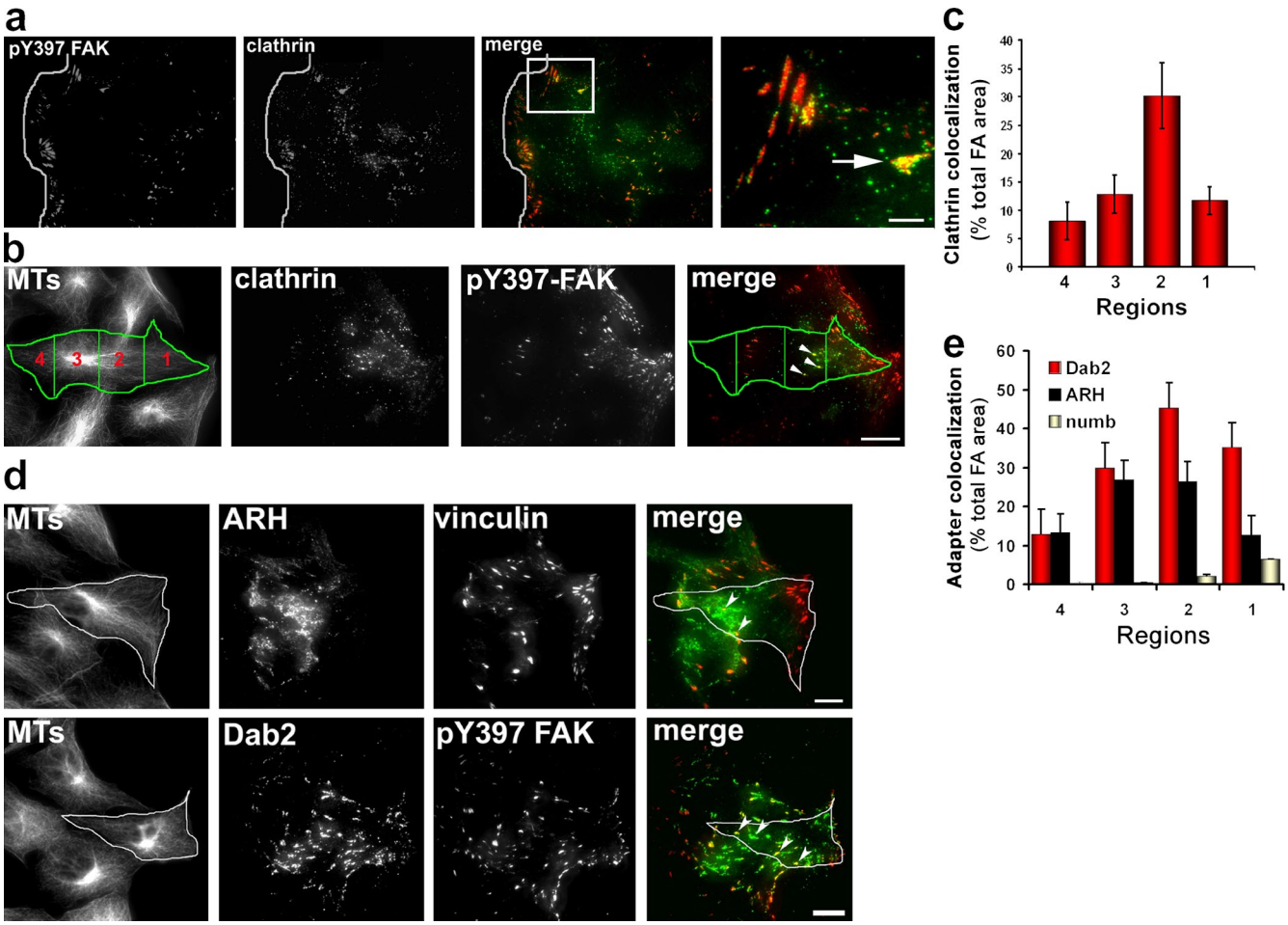


Figure 6. **Clathrin and adaptor protein localization during polarized cell migration.** (a) TIRF image of an NIH3T3 fibroblast migrating into an in vitro wound immunostained with antibodies against pY397 FAK and clathrin. The white line shows the wound edge. The merge image shows pY397 FAK (red) and clathrin (green). The boxed region in the merge image is shown at higher magnification on the right. The arrow indicates a focal adhesion located behind the leading edge that has accumulated clathrin puncta. (b) Representative images used for quantitative colocalization of clathrin and focal adhesions in different regions of an NIH3T3 fibroblast migrating into an in vitro wound and immunostained with antibodies against MTs, pY397 FAK, and clathrin. The MT image shows the cell outline and four regions used for quantification (see Materials and methods). The merged image shows pY397 FAK (red) and clathrin heavy chain (green) and the four regions. Arrowheads indicate focal adhesions that colocalize with clathrin puncta. (c) Quantification of focal adhesion (FA) area that colocalizes with clathrin puncta in the four regions defined in b. The histogram represents data from two independent experiments in which 15–20 individual cells were analyzed. (d) Images of NIH3T3 fibroblasts migrating into an in vitro wound and immunostained for MTs, vinculin or pY397 FAK, and ARH or Dab2. The merged images at right show pY397 FAK or vinculin (red) and ARH or Dab2 (green). An individual migrating cell at the wound edge is indicated by the outline. Arrowheads indicate focal adhesions that colocalized with either ARH or Dab2 puncta. (e) Quantification of adaptor protein colocalization with focal adhesion area in the four regions defined in b. The histogram represents data from two independent experiments in which colocalization was measured in 10–20 individual cells. (c and e) Error bars are SEM. Bars, 15 µm.

### Clathrin and its adaptors contribute to focal adhesion disassembly in migrating cells

To determine whether clathrin and its adaptors are important for focal adhesion disassembly in a physiological context, we depleted clathrin, Dab2, and ARH using siRNA and tested the ability of these cells to migrate into a wounded monolayer. Clathrin and Dab2 have previously been implicated in cell migration (Hocevar et al., 2005; Nishimura and Kaibuchi, 2007; Chao and Kunz, 2009), and we confirmed that cells depleted of these proteins were impaired in directed migration into an in vitro wound (Fig. 7, a and b). Depletion of ARH, which has not previously been studied in cell migration, also inhibited directed cell migration (Fig. 7, a and b). Simultaneous depletion of both Dab2 and ARH inhibited migration to a greater extent than individual depletion of the proteins and similar to that in clathrin-depleted cells (Fig. 7 b). These results parallel our finding that depletion of both adaptor proteins was necessary to significantly inhibit MT-induced focal adhesion disassembly. Migrating cells depleted of clathrin or both clathrin adaptors also exhibited elongated tails (Fig. 7, c and d). This phenotype is characteristic of defective focal adhesion disassembly and had not been previously reported in other studies investigating the role of Dab2 and clathrin during cell migration. To determine whether inhibition of cell migration was related to defects in focal adhesion disassembly, we analyzed focal adhesion disassembly in migrating cells stably expressing GFP-FAK (Partridge and Marcantonio, 2006) and depleted of clathrin or ARH and Dab2. We found that overall focal adhesion disassembly was reduced by 60–70% in cells depleted of clathrin or ARH and Dab2 (Fig. 7, e and f). These

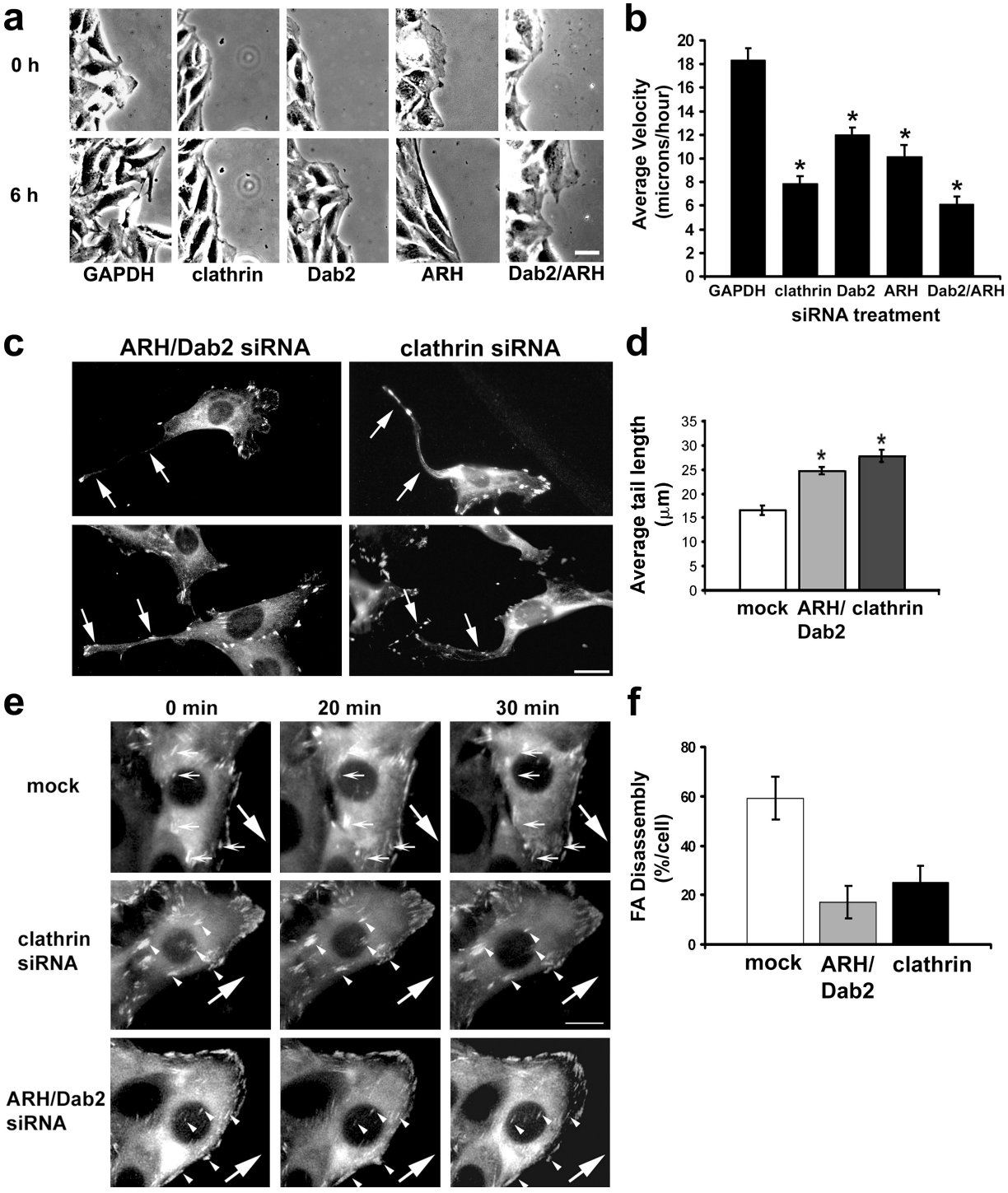


Figure 7. **Clathrin and clathrin adaptors are required for focal adhesion disassembly and polarized cell migration.** (a) Phase images from videos of NIH3T3 cells treated with the indicated siRNA and allowed to migrate into a wound. The same wound edge is shown at 0 and 6 h of migration. (b) Quantification of wound migration velocity of cells depleted of clathrin or clathrin adaptors. The histogram represents two to three independent experiments in which 20 wounds were analyzed per condition. *, $P \leq 0.0001$ for each condition compared with GAPDH by Student's *t* test. (c) Immunofluorescence of NIH3T3 cells depleted of either clathrin or Dab2 and ARH and immunostained for vinculin. Cells were allowed to migrate into a wound for 9 h before processing for immunofluorescence. Arrows indicate examples of elongated tails. (d) Quantification of tail length in migrating cells depleted of clathrin or clathrin adaptors. The histogram represents two independent experiments in which at least 20 cells were analyzed per condition. *, $P \leq 0.005$ for each condition compared with mock by Student's *t* test. (e) Fluorescence images from videos of migrating NIH3T3 cells stably expressing GFP-FAK and depleted of clathrin, Dab2, and ARH or mock treated (0-, 20-, or 30-min time points are shown). Small arrows point to focal adhesions that disassemble during 30 min of cell migration. Arrowheads point to focal adhesions that fail to disassemble during 30 min of cell migration. Large arrows indicate the direction of migration. (f) Quantitative analysis of focal adhesion (FA) disassembly in cells depleted of clathrin or ARH and Dab2. The histogram shows the percentage of focal adhesions that disassemble per cell during a 30-min interval. For each of the conditions analyzed, focal adhesion disassembly was quantified for at least 10 different cells (30–50 adhesions per cell) from five to eight separate videos. (b, d, and f) Error bars are SEM. Bars, 15 μm.

results are consistent with the idea that clathrin and its adaptors Dab2 and ARH play an important role in focal adhesion disassembly during directed cell migration.

## Discussion

We have shown that MT-induced focal adhesion disassembly occurs via the direct endocytosis of integrin at focal adhesions mediated by clathrin. It has been suggested that general loss of contractility is the primary mechanism by which focal adhesions disassemble in response to MT targeting (Kaverina et al., 2002). However, our data indicate that MT-induced focal adhesion disassembly is mediated by a hierarchical assembly of endocytic components at the focal adhesion, which then induce disassembly by mediating endocytosis of integrins. TIRF imaging data support the direct endocytosis of integrin by clathrin because we observed the simultaneous disappearance of clathrin and integrin during disassembly, although we cannot rule out that some integrin is disassembled through other processes. Our current results, coupled with earlier results showing the dynamin dependence and Rho independence of focal adhesion disassembly (Ezratty et al., 2005), strengthen the idea that focal adhesion disassembly is mechanistically distinct from focal adhesion formation.

The factors involved in integrin endocytosis have been unexplored until recently. Our study points to clathrin and its adaptors Dab2 and ARH as key participants in integrin endocytosis. The weaker inhibition of focal adhesion disassembly and integrin endocytosis in Dab2/ARH compared with clathrin-depleted cells suggests that there may be additional adaptors involved in clathrin-mediated disassembly of focal adhesions. In fact, while our paper was under review, another paper reported that Dab2 and AP-2 were involved in focal adhesion disassembly and integrin endocytosis in human fibrosarcoma cells (Chao and Kunz, 2009). We did not observe AP-2 localization to focal adhesions or inhibition of disassembly with dominant-negative AP-2 constructs, suggesting that AP-2 is not generally involved in focal adhesion disassembly. Studies on HeLa cells have suggested that numb and Dab2 participate in integrin endocytosis, although in these studies, the internalized integrin was not likely to be engaged and in focal adhesions (Nishimura and Kaibuchi, 2007; Teckchandani et al., 2009). There is also evidence that non-ECM–engaged integrin can be endocytosed by a clathrin-independent, caveolin-dependent pathway (Fabbri et al., 2005; Echarri and Del Pozo, 2006). Together, these studies point to a degree of complexity in integrin endocytosis in which it is possible that different adaptors are used for different integrins or for the same integrin but in different states of engagement with the ECM.

The accumulation of clathrin and its adaptors at focal adhesions provides a way to temporally and spatially regulate focal adhesion disassembly during cell migration and suggests that focal adhesions are more heterogeneous structures than had previously been appreciated. We found that both clathrin and its adaptors Dab2 and ARH were required for focal adhesion disassembly and localized to focal adhesions in specific regions of migrating fibroblasts. Interestingly, Dab2 and ARH were observed at more focal adhesions than clathrin, suggesting that Dab2 and ARH may precede clathrin at focal adhesions or that clathrin may not persist for long before focal adhesion disassembly commences. Additional imaging studies will be needed to ascertain the dynamic relationship between Dab2, ARH, and clathrin at disassembling focal adhesions.

How might clathrin and its adaptors target focal adhesions for their disassembly? Previous studies have shown that more mature focal adhesions accumulate late focal adhesion proteins such as α-actinin (Laukaitis et al., 2001) and have higher levels of tyrosine phosphorylated focal adhesion components (Zamir et al., 1999). The accumulation of clathrin or its adaptors at focal adhesions may be caused by these or other maturation processes at focal adhesions. MTs may also contribute to the accumulation by rapidly directing clathrin and/or its adaptors to focal adhesions. Once clathrin and its adaptors accumulate at focal adhesions, they may stimulate endocytosis not only by recruiting clathrin but by competing with existing interactions between focal adhesion components and integrin. For example, Dab2 may compete with talin for NPXY-binding sites, and this could decrease integrin–ECM engagement by reversing integrin activation and/or releasing integrin from its primary connection to the actin cytoskeleton.

It is well established that MTs are not required for endocytosis per se, and it has been suggested that MTs likely deliver a relaxing factor to focal adhesions that may facilitate their disassembly (Kaverina et al., 2002). Both clathrin and Dab2 accumulated slowly (over hours) at focal adhesions in the absence of MTs, indicating that MTs are not absolutely required for their targeting to focal adhesions. However, a much more rapid accumulation (in minutes) of clathrin at focal adhesions occurred during MT-induced focal adhesion disassembly, suggesting that MTs may facilitate the targeting of clathrin to focal adhesions. The rapid accumulation of clathrin may reflect delivery of clathrin by MTs as clathrin puncta have been seen traveling along MTs near the plasma membrane (Rappoport et al., 2003). The possibility that Dab2 or ARH move along MTs has not yet been explored. Alternatively, MTs may regulate the accumulation of clathrin or its adaptors at focal adhesions indirectly by regulating binding sites for these proteins at the focal adhesion. It will be interesting to determine the mechanism by which MTs enhance clathrin and perhaps other endocytic protein targeting to focal adhesions during disassembly.

## Materials and methods

### Chemicals and cell culture

All chemicals were purchased from Sigma-Aldrich unless otherwise noted. NIH3T3 fibroblasts were cultured in DME and calf serum as previously described (Ezratty et al., 2005). HA1 cells (NIH3T3 fibroblasts engineered to express human α1 integrin) were cultured in DME, calf serum, and 300 μg/ml G418 as previously described (Briesewitz et al., 1993). For serum starvation, cells on acid-washed coverslips were grown to confluence (~2 d) and transferred to serum-free medium (DME and 10 mM Hepes, pH 7.4) for 48 h as previously described (Ezratty et al., 2005). shDab2 pools and clonal cell lines were derived as previously described (Prunier and Howe, 2005) except NIH3T3 fibroblasts were cotransfected with the shDab2 construct (provided by P. Howe, Lerner Research Institute, Cleveland, OH) and pcDNA3.1 Zeo and then selected using 500 μg/ml Zeocin (Invitrogen).

### Focal adhesion disassembly and cell migration experiments

Focal adhesion disassembly and cell migration experiments were performed as previously described (Ezratty et al., 2005). In brief, NIH3T3

cells grown on glass coverslips were treated with 10 µM nocodazole for 3–4 h to completely depolymerize MTs. The drug was washed out with serum-free medium, and MTs were allowed to repolymerize for different intervals. Cells were either fixed in −20°C methanol for 10 min and rehydrated in TBS or fixed in 4% paraformaldehyde in PBS for 10 min, followed by permeabilization with 0.5% Triton X-100 in PBS for 5 min before immunofluorescence staining. Depending on the experiment, cells were stained with vinculin (mouse monoclonal; 1:100; Sigma-Aldrich), pY397 FAK (rabbit polyclonal; 1:100; Invitrogen), zyxin (1:100; Sigma-Aldrich), dynamin (hudy-1; 1:100; Millipore), clathrin (TD.1 [1:50; BD] or X22 [1:100; Abcam]), AP-2 (1:100; α-adaptin subunit; Abcam), Dab2/p96 (mouse monoclonal; 1:100; BD), ARH (rabbit polyclonal; 1:800; provided by M. Farquhar, University of California, San Diego, La Jolla, CA), numb (1:100; Santa Cruz Biotechnology, Inc.), β1 integrin (1:100; BD), tyrosinated tubulin (rat monoclonal YL1/2; 1:10 dilution of culture supernatant), or Cy5/rhodamine-phalloidin (1:200 dilution; Cytoskeleton, Inc.). Secondary antibodies were purchased from Jackson ImmunoResearch Laboratories, Inc. and were absorbed to minimize cross-reaction with other species.

**Clathrin inhibition and RabQ79L experiments**

NIH3T3 cells were transfected with FKBP–clathrin LC–GFP (provided by T. Ryan, Cornell University, New York, NY; Moskowitz et al., 2003) or Rab5Q79L (provided by J. Lippincott-Schwartz, National Institutes of Health, Bethesda, MD; Stenmark et al., 1994) with Lipofectamine Plus (Invitrogen) according to the manufacturer's instructions. After 24–48 h of transfection, cells were treated with 10 µM nocodazole for 4 h, and then focal adhesion disassembly was stimulated via MT regrowth. For clathrin inhibition, 100 nM AP20187 (ARIAD) was added to FKBP–clathrin LC–GFP-transfected cells for 30 min before nocodazole washout and during MT regrowth. For transferrin internalization, cells were incubated at 37° with 10 µg/ml Alexa Fluor 546–labeled transferrin (Invitrogen) for 10 min. Remaining plasma membrane–bound transferrin was removed by incubating cells for 2 min with 0.5 M NaCl and 0.2 M of Na acetate buffer, pH 4.5, followed by washing with the same solution before processing for immunofluorescence.

**siRNA knockdown experiments**

RNA duplexes (21 nucleotides) were purchased from Invitrogen or Shanghai GenePharma and resuspended in RNAase-free water at a concentration of 20 µM. siRNAs were designed based on previously published sequences (Hocevar et al., 2005; Moskowitz et al., 2005) as follows: clathrin-1, 5′-AACAUUGGCUUCAGUACCUUGTT-3′; clathrin-2, 5′-AAUGGAUCUCUUUGAAUACGGTT-3′; Dab2-1, 5′-GAACGGCUUCCAUAUCAAATT-3′; Dab2-2, 5′-CGUCUACUCCACAGAGUAATT-3′; ARH-1, 5′-CCTGCTGGATTTGGAAGAGTT-3′; ARH-2, 5′-GTTGCCAGAGAACTGGACGTT-3′; numb-1, 5′-CGUAGAAGUUGAUGAGUCATT-3′; and numb-2, 5′-AGAAGAUGUCACCCUUUAATT-3′. The mouse GAPDH siRNA sequence was 5′-AAAGUUGUCAUGGAUGACCTT-3′ and was used as a negative control in all siRNA experiments. For some experiments, Dab2 and ARH were knocked down simultaneously by treating with both siRNAs. NIH3T3 fibroblasts were transfected with siRNA duplexes using Lipofectamine RNAiMax (Invitrogen) according to the manufacturer's instructions for reverse transfection. Optimal knockdown for all proteins was obtained by two transfections spaced 48 h apart. Knockdown efficiency and effects on focal adhesion disassembly and transferrin uptake were analyzed 24–48 h after the last transfection.

**Western blotting**

Cells were lysed in lysis buffer (1% NP-40, 50 mM Tris, pH 7.4, 150 mM NaCl, 2 mM $MgCl_2$, 1 mM EGTA, and protease and phosphatase inhibitors), boiled in 2× Laemmli sample buffer, and then separated by SDS-PAGE on 7.5 or 10% gels. Lysate protein concentration was determined by bicinchoninic acid assay and normalized for loading. Gels were transferred to nitrocellulose, blocked 1 h at room temperature in TBS buffer containing 5% BSA, and then incubated in 5% BSA/TBST overnight at 4°C with antibodies against clathrin heavy chain (1:500; TD.1), Dab2 (1:2,000), ARH (1:2,000), pY397 FAK (1:5,000), vinculin (1:5000), or tubulin (1:100,000; rabbit polyclonal tyrosinated tubulin $W^2$) followed by the appropriate IR680- or IR800-conjugated secondary antibodies (1:5,000; Rockland Immunochemicals, Inc.). Quantification of bands was performed with an Odyssey imaging system (LI-COR Biosciences).

**Epifluorescence and TIRF microscopy**

Immunofluorescently stained preparations were observed with a microscope (Optiphot; Nikon) using a 60× Plan-Apochromat objective and filter cubes optimized for coumarin, fluorescein/GFP, rhodamine, and Cy5 fluorescence. Images were captured with a camera (Kodak KAF 1,400-chip MicroMax; Princeton Instruments) using MetaMorph software (MDS Analytical Technologies). For TIRF microscopy, preparations were observed using a 60× NA 1.45 Apochromat objective on a microscope (TE2000-U; Nikon) equipped with a TIRF illuminator and fiber optic–coupled laser illumination. Illumination was performed with three separate laser lines (Ar ion [488 nm] and HeNe [543 nm and 633 nm]) and filter cubes optimized for fluorescein/GFP, Cy3/Alexa Fluor 546, and Cy5 fluorescence (Chroma Technology Corp.). Images were captured with a camera (OrcaIIER; Hamamatsu Photonics) using MetaMorph software. For live cell imaging of clathrin and FAK, stable NIH3T3 cell lines expressing GFP–clathrin LC (provided by C. Waterman-Storer, National Institutes of Health) were generated as previously described (Merrifield et al., 2002) and transiently transfected with RFP-FAK (Partridge and Marcantonio, 2006) for 24–48 h before TIRF imaging. Images of RFP-FAK and GFP-clathrin were acquired every 60 s. For live cell imaging of integrin and clathrin, stable NIH3T3 cell lines expressing low levels of a GFP–β1 integrin chimera (Smilenov et al., 1999) were transiently transfected with DsRed–clathrin LC (Merrifield et al., 2002) for 24–48 h. Images of GFP—β1 integrin and -clathrin were acquired every 20–60 s. Imaging was performed at 37°C in recording media (Gomes and Gundersen, 2006) and started within 15 min of MT regrowth.

For imaging cell migration, monolayers of cells transfected with siRNAs were wounded and imaged in recording media supplemented with 2% calf serum. Multiple fields were imaged every 30 min for 9–12 h using an XY stage (Prior) and a 60× NA 0.6 Plan-Fluor objective (Nikon). Phase-contrast images were collected with a camera (CoolSNAP HQ; Roper Industries) controlled by MetaMorph. For analysis of focal adhesion dynamics, monolayers of NIH3T3 cells stably expressing GFP-FAK (Partridge and Marcantonio, 2006) and transfected with siRNAs were imaged as described above, except that multiple fields were imaged every 10 min for 2–3 h.

**Quantitative immunofluorescence and image processing**

The MetaMorph measure colocalization function was used to quantify colocalization of focal adhesions and clathrin or adaptor proteins and colocalization of integrin and Rab5Q79L endosomes. Each source image was equally thresholded to obtain just focal adhesion, clathrin, or adaptor protein staining before measuring the extent of colocalization. For colocalization experiments in migrating cells, the length of the wound edge cells was measured from tail to front, and the perimeter was determined by manually tracing an outline of the cell. This entire area was then divided into four equal regions along the front to back axis. A region tool was used to select a specific region of interest (labeled as quadrants 1–4) for the measurement of clathrin or adaptor and focal adhesion (detected with FAK-Y397 or vinculin) colocalization. For analysis of focal adhesion disassembly during cell migration, individual focal adhesions were equally thresholded and monitored for their disappearance or maintenance within a 30-min interval during cell migration. For plots of clathrin colocalization during focal adhesion disassembly, the region tool was used to outline a given focal adhesion, and its area was determined in sequential images during MT-induced focal adhesion disassembly. The measure colocalization function was then used to determine the area of overlap between the focal adhesion and clathrin. To measure the size or number of focal adhesions, fluorescent images of individual cells were thresholded, and the measurement function in MetaMorph was used to calculate the area and number of objects. To analyze the length of tails in migrating cells, a line was drawn from the end of the tail to the back of the nucleus, and the total length of the line was determined. For all images shown, the brightness and contrast were first optimized and appropriately scaled in MetaMorph before importing into Photoshop (Adobe) for the preparation of figures.

**Cell surface labeling and flow cytometry**

Cells were harvested by trypsinization at time points after MT regrowth and washed in cold PCN (1× PBS, 0.5% calf serum, and 0.1% $NaN_3$). Approximately $4 \times 10^6$ cells per sample were stained at 4°C without fixation. For the detection of α5 integrin in NIH3T3 and HA1 fibroblasts, PE-conjugated rat α-mouse CD49e monoclonal antibody (BD) was used at dilution of 1:1500. For the detection of α1 integrin in HA1 cells, mouse α-human TS2/7 monoclonal antibody (gift from T. Springer, Harvard University, Cambridge, MA) was used at a dilution of 1:200, followed by 1:500 dilution of FITC α-mouse IgG (Jackson ImmunoResearch Laboratories, Inc.). After washes to remove unbound antibody, samples were fixed in cold 4% paraformaldehyde/PCN, and the distribution and mean fluorescence intensity of each sample was quantified using a FACScan (BD).

### Statistical analysis

Where indicated, data were analyzed using the Student's *t* test.

### Online supplemental material

Fig. S1 shows that clathrin knockdown prevents focal adhesion disassembly and transferrin internalization compared with mock-transfected cells. Fig. S2 shows the total surface α5 or β1 integrin levels before and after MT-induced focal adhesion disassembly. Fig. S3 shows that clathrin accumulates at focal adhesions during nocodazole treatment. Fig. S4 shows that the expression of Eps15Δ95-295 inhibits transferrin uptake but not focal adhesion disassembly. Fig. S5 shows the localization of clathrin and clathrin adaptor proteins in cells depleted of Dab2. Online supplemental material is available at http://www.jcb.org/cgi/content/full/jcb.200904054/DC1.

E.E. Marcantonio would like to dedicate this paper to the memory of Dr. Tucker Collins.

We thank G. DiPaolo and members of the Gundersen laboratory for critically reading the manuscript. M. Partridge and the staff of the flow cytometry core facility at Columbia University assisted with analyses. We are indebted to M. Farquhar for ARH constructs and antibodies, P. Howe for the shDab2 plasmid, and T. Ryan for the FKBP–clathrin LC–GFP. The TS2/7 antibody was from T. Springer, the Rab5Q79L-EGFP and Eps15 plasmids were gifts from J. Lippincott-Schwartz, and the GFP–clathrin LC construct was provided by C. Waterman-Storer.

This work is supported by National Institutes of Health grant GM68595 (to G.G. Gundersen).

Submitted: 10 April 2009
Accepted: 3 November 2009

## References

Abercrombie, M. 1980. The crawling behavior of metazoan cells. *Proc. R. Soc. Lond. B. Biol. Sci.* 207:129–147. doi:10.1098/rspb.1980.0017

Benmerah, A., V. Poupon, N. Cerf-Bensussan, and A. Dautry-Varsat. 2000. Mapping of Eps15 domains involved in its targeting to clathrin-coated pits. *J. Biol. Chem.* 275:3288–3295. doi:10.1074/jbc.275.5.3288

Briesewitz, R., A. Kern, and E.E. Marcantonio. 1993. Ligand-dependent and -independent integrin focal contact localization: the role of the alpha chain cytoplasmic domain. *Mol. Biol. Cell*. 4:593–604.

Bruzzaniti, A., L. Neff, A. Sanjay, W.C. Horne, P. De Camilli, and R. Baron. 2005. Dynamin forms a Src kinase-sensitive complex with Cbl and regulates podosomes and osteoclast activity. *Mol. Biol. Cell*. 16:3301–3313. doi:10.1091/mbc.E04-12-1117

Burridge, K. 2005. Foot in mouth: do focal adhesions disassemble by endocytosis? *Nat. Cell Biol.* 7:545–547. doi:10.1038/ncb0505-545

Calderwood, D.A., Y. Fujioka, J.M. de Pereda, B. García-Alvarez, T. Nakamoto, B. Margolis, C.J. McGlade, R.C. Liddington, and M.H. Ginsberg. 2003. Integrin beta cytoplasmic domain interactions with phosphotyrosine-binding domains: a structural prototype for diversity in integrin signaling. *Proc. Natl. Acad. Sci. USA*. 100:2272–2277. doi:10.1073/pnas.262791999

Caswell, P.T., and J.C. Norman. 2006. Integrin trafficking and the control of cell migration. *Traffic*. 7:14–21. doi:10.1111/j.1600-0854.2005.00362.x

Chao, W.T., and J. Kunz. 2009. Focal adhesion disassembly requires clathrin-dependent endocytosis of integrins. *FEBS Lett.* 583:1337–1343. doi:10.1016/j.febslet.2009.03.037

Clackson, T., W. Yang, L.W. Rozamus, M. Hatada, J.F. Amara, C.T. Rollins, L.F. Stevenson, S.R. Magari, S.A. Wood, N.L. Courage, et al. 1998. Redesigning an FKBP-ligand interface to generate chemical dimerizers with novel specificity. *Proc. Natl. Acad. Sci. USA*. 95:10437–10442. doi:10.1073/pnas.95.18.10437

Echarri, A., and M.A. Del Pozo. 2006. Caveolae internalization regulates integrin-dependent signaling pathways. *Cell Cycle*. 5:2179–2182.

Ehrlich, M., W. Boll, A. Van Oijen, R. Hariharan, K. Chandran, M.L. Nibert, and T. Kirchhausen. 2004. Endocytosis by random initiation and stabilization of clathrin-coated pits. *Cell*. 118:591–605. doi:10.1016/j.cell.2004.08.017

Ezratty, E.J., M.A. Partridge, and G.G. Gundersen. 2005. Microtubule-induced focal adhesion disassembly is mediated by dynamin and focal adhesion kinase. *Nat. Cell Biol.* 7:581–590. doi:10.1038/ncb1262

Fabbri, M., S. Di Meglio, M.C. Gagliani, E. Consonni, R. Molteni, J.R. Bender, C. Tacchetti, and R. Pardi. 2005. Dynamic partitioning into lipid rafts controls the endo-exocytic cycle of the alphaL/beta2 integrin, LFA-1, during leukocyte chemotaxis. *Mol. Biol. Cell*. 16:5793–5803. doi:10.1091/mbc.E05-05-0413

Gomes, E.R., and G.G. Gundersen. 2006. Real-time centrosome reorientation during fibroblast migration. *Methods Enzymol.* 406:579–592. doi:10.1016/S0076-6879(06)06045-9

Gupton, S.L., and C.M. Waterman-Storer. 2006. Spatiotemporal feedback between actomyosin and focal-adhesion systems optimizes rapid cell migration. *Cell*. 125:1361–1374. doi:10.1016/j.cell.2006.05.029

Hendey, B., C.B. Klee, and F.R. Maxfield. 1992. Inhibition of neutrophil chemokinesis on vitronectin by inhibitors of calcineurin. *Science*. 258:296–299. doi:10.1126/science.1384129

Hocevar, B.A., C. Prunier, and P.H. Howe. 2005. Disabled-2 (Dab2) mediates transforming growth factor beta (TGFbeta)-stimulated fibronectin synthesis through TGFbeta-activated kinase 1 and activation of the JNK pathway. *J. Biol. Chem.* 280:25920–25927. doi:10.1074/jbc.M501150200

Kaverina, I., O. Krylyshkina, and J.V. Small. 1999. Microtubule targeting of substrate contacts promotes their relaxation and dissociation. *J. Cell Biol.* 146:1033–1044. doi:10.1083/jcb.146.5.1033

Kaverina, I., O. Krylyshkina, and J.V. Small. 2002. Regulation of substrate adhesion dynamics during cell motility. *Int. J. Biochem. Cell Biol.* 34:746–761. doi:10.1016/S1357-2725(01)00171-6

Keyel, P.A., S.K. Mishra, R. Roth, J.E. Heuser, S.C. Watkins, and L.M. Traub. 2006. A single common portal for clathrin-mediated endocytosis of distinct cargo governed by cargo-selective adaptors. *Mol. Biol. Cell*. 17:4300–4317. doi:10.1091/mbc.E06-05-0421

Kopp, P., R. Lammers, M. Aepfelbacher, G. Woehlke, T. Rudel, N. Machuy, W. Steffen, and S. Linder. 2006. The kinesin KIF1C and microtubule plus ends regulate podosome dynamics in macrophages. *Mol. Biol. Cell*. 17:2811–2823. doi:10.1091/mbc.E05-11-1010

Lauffenburger, D.A., and A.F. Horwitz. 1996. Cell migration: a physically integrated molecular process. *Cell*. 84:359–369. doi:10.1016/S0092-8674(00)81280-5

Laukaitis, C.M., D.J. Webb, K. Donais, and A.F. Horwitz. 2001. Differential dynamics of α5 integrin, paxillin, and α-actinin during formation and disassembly of adhesions in migrating cells. *J. Cell Biol.* 153:1427–1440. doi:10.1083/jcb.153.7.1427

Lawson, M.A., and F.R. Maxfield. 1995. Ca(2+)- and calcineurin-dependent recycling of an integrin to the front of migrating neutrophils. *Nature*. 377:75–79. doi:10.1038/377075a0

Merrifield, C.J., M.E. Feldman, L. Wan, and W. Almers. 2002. Imaging actin and dynamin recruitment during invagination of single clathrin-coated pits. *Nat. Cell Biol.* 4:691–698. doi:10.1038/ncb837

Moskowitz, H.S., J. Heuser, T.E. McGraw, and T.A. Ryan. 2003. Targeted chemical disruption of clathrin function in living cells. *Mol. Biol. Cell*. 14:4437–4447. doi:10.1091/mbc.E03-04-0230

Moskowitz, H.S., C.T. Yokoyama, and T.A. Ryan. 2005. Highly cooperative control of endocytosis by clathrin. *Mol. Biol. Cell*. 16:1769–1776. doi:10.1091/mbc.E04-08-0739

Nishimura, T., and K. Kaibuchi. 2007. Numb controls integrin endocytosis for directional cell migration with aPKC and PAR-3. *Dev. Cell*. 13:15–28. doi:10.1016/j.devcel.2007.05.003

Palecek, S.P., C.E. Schmidt, D.A. Lauffenburger, and A.F. Horwitz. 1996. Integrin dynamics on the tail region of migrating fibroblasts. *J. Cell Sci.* 109:941–952.

Palecek, S.P., J.C. Loftus, M.H. Ginsberg, D.A. Lauffenburger, and A.F. Horwitz. 1997. Integrin-ligand binding properties govern cell migration speed through cell-substratum adhesiveness. *Nature*. 385:537–540. doi:10.1038/385537a0

Palecek, S.P., A. Huttenlocher, A.F. Horwitz, and D.A. Lauffenburger. 1998. Physical and biochemical regulation of integrin release during rear detachment of migrating cells. *J. Cell Sci.* 111:929–940.

Partridge, M.A., and E.E. Marcantonio. 2006. Initiation of attachment and generation of mature focal adhesions by integrin-containing filopodia in cell spreading. *Mol. Biol. Cell*. 17:4237–4248. doi:10.1091/mbc.E06-06-0496

Pellinen, T., and J. Ivaska. 2006. Integrin traffic. *J. Cell Sci.* 119:3723–3731. doi:10.1242/jcs.03216

Pellinen, T., A. Arjonen, K. Vuoriluoto, K. Kallio, J.A. Fransen, and J. Ivaska. 2006. Small GTPase Rab21 regulates cell adhesion and controls endosomal traffic of β1-integrins. *J. Cell Biol.* 173:767–780. doi:10.1083/jcb.200509019

Pierini, L.M., M.A. Lawson, R.J. Eddy, B. Hendey, and F.R. Maxfield. 2000. Oriented endocytic recycling of alpha5beta1 in motile neutrophils. *Blood*. 95:2471–2480.

Prunier, C., and P.H. Howe. 2005. Disabled-2 (Dab2) is required for transforming growth factor beta-induced epithelial to mesenchymal transition (EMT). *J. Biol. Chem.* 280:17540–17548. doi:10.1074/jbc.M500974200

Puthenveedu, M.A., and M. von Zastrow. 2006. Cargo regulates clathrin-coated pit dynamics. *Cell*. 127:113–124. doi:10.1016/j.cell.2006.08.035

Rappoport, J.Z., B.W. Taha, and S.M. Simon. 2003. Movement of plasma-membrane-associated clathrin spots along the microtubule cytoskeleton. *Traffic*. 4:460–467. doi:10.1034/j.1600-0854.2003.00100.x

Ridley, A.J., M.A. Schwartz, K. Burridge, R.A. Firtel, M.H. Ginsberg, G. Borisy, J.T. Parsons, and A.R. Horwitz. 2003. Cell migration: integrating signals from front to back. *Science*. 302:1704–1709. doi:10.1126/science.1092053

Roberts, M., S. Barry, A. Woods, P. van der Sluijs, and J. Norman. 2001. PDGF-regulated rab4-dependent recycling of alphavbeta3 integrin from early endosomes is necessary for cell adhesion and spreading. *Curr. Biol.* 11:1392–1402. doi:10.1016/S0960-9822(01)00442-0

Rottner, K., A. Hall, and J.V. Small. 1999. Interplay between Rac and Rho in the control of substrate contact dynamics. *Curr. Biol.* 9:640–648. doi:10.1016/S0960-9822(99)80286-3

Sastry, S.K., and K. Burridge. 2000. Focal adhesions: a nexus for intracellular signaling and cytoskeletal dynamics. *Exp. Cell Res.* 261:25–36. doi:10.1006/excr.2000.5043

Smilenov, L.B., A. Mikhailov, R.J. Pelham, E.E. Marcantonio, and G.G. Gundersen. 1999. Focal adhesion motility revealed in stationary fibroblasts. *Science*. 286:1172–1174. doi:10.1126/science.286.5442.1172

Stenmark, H., R.G. Parton, O. Steele-Mortimer, A. Lütcke, J. Gruenberg, and M. Zerial. 1994. Inhibition of rab5 GTPase activity stimulates membrane fusion in endocytosis. *EMBO J.* 13:1287–1296.

Teckchandani, A., N. Toida, J. Goodchild, C. Henderson, J. Watts, B. Wollscheid, and J.A. Cooper. 2009. Quantitative proteomics identifies a Dab2/integrin module regulating cell migration. *J. Cell Biol.* 186:99–111. doi:10.1083/jcb.200812160

Traub, L.M. 2003. Sorting it out: AP-2 and alternate clathrin adaptors in endocytic cargo selection. *J. Cell Biol.* 163:203–208. doi:10.1083/jcb.200309175

Uhlik, M.T., B. Temple, S. Bencharit, A.J. Kimple, D.P. Siderovski, and G.L. Johnson. 2005. Structural and evolutionary division of phosphotyrosine binding (PTB) domains. *J. Mol. Biol.* 345:1–20. doi:10.1016/j.jmb.2004.10.038

Webb, D.J., J.T. Parsons, and A.F. Horwitz. 2002. Adhesion assembly, disassembly and turnover in migrating cells — over and over and over again. *Nat. Cell Biol.* 4:E97–E100. doi:10.1038/ncb0402-e97

Webb, D.J., K. Donais, L.A. Whitmore, S.M. Thomas, C.E. Turner, J.T. Parsons, and A.F. Horwitz. 2004. FAK-Src signalling through paxillin, ERK and MLCK regulates adhesion disassembly. *Nat. Cell Biol.* 6:154–161. doi:10.1038/ncb1094

Worthylake, R.A., S. Lemoine, J.M. Watson, and K. Burridge. 2001. RhoA is required for monocyte tail retraction during transendothelial migration. *J. Cell Biol.* 154:147–160. doi:10.1083/jcb.200103048

Yeo, M.G., M.A. Partridge, E.J. Ezratty, Q. Shen, G.G. Gundersen, and E.E. Marcantonio. 2006. Src SH2 arginine 175 is required for cell motility: specific focal adhesion kinase targeting and focal adhesion assembly function. *Mol. Cell. Biol.* 26:4399–4409. doi:10.1128/MCB.01147-05

Zamir, E., B.Z. Katz, S. Aota, K.M. Yamada, B. Geiger, and Z. Kam. 1999. Molecular diversity of cell-matrix adhesions. *J. Cell Sci.* 112:1655–1669.